12928–12938 *Nucleic Acids Research, 2014, Vol. 42, No. 20* *Published online 16 October 2014*
doi: 10.1093/nar/gku962

A nanobody modulates the p53 transcriptional program without perturbing its functional architecture

Jonas Bethuyne[1], Steven De Gieter[2], Olivier Zwaenepoel[1], Abel Garcia-Pino[2], Kaat Durinck[3], Adriaan Verhelle[1], Gholamreza Hassanzadeh-Ghassabeh[4], Frank Speleman[3], Remy Loris[2] and Jan Gettemans[1,*]

[1]Nanobody Lab, Department of Biochemistry, Ghent University, Albert Baertsoenkaai 3, B-9000 Ghent, Belgium, [2]Structural Biology Brussels, Department of Biotechnology, Vrije Universiteit Brussel and Structural Biology Research Center, Vlaams Instituut voor Biotechnologie (VIB), Pleinlaan 2, B-1050 Brussel, Belgium, [3]Center for Medical Genetics, Ghent University Hospital, De Pintelaan 185, B-9000 Ghent, Belgium and [4]Nanobody Service Facility, Vlaams Instituut voor Biotechnologie (VIB), Pleinlaan 2, B-1050 Brussels, Belgium

Received June 18, 2014; Revised September 29, 2014; Accepted September 30, 2014

ABSTRACT

The p53 transcription factor plays an important role in genome integrity. To perform this task, p53 regulates the transcription of genes promoting various cellular outcomes including cell cycle arrest, apoptosis or senescence. The precise regulation of this activity remains elusive as numerous mechanisms, e.g. posttranslational modifications of p53 and (non-)covalent p53 binding partners, influence the p53 transcriptional program. We developed a novel, non-invasive tool to manipulate endogenous p53. Nanobodies (Nb), raised against the DNA-binding domain of p53, allow us to distinctively target both *wild type* and mutant p53 with great specificity. Nb3 preferentially binds 'structural' mutant p53, i.e. R175H and R282W, while a second but distinct nanobody, Nb139, binds both mutant and *wild type* p53. The co-crystal structure of the p53 DNA-binding domain in complex with Nb139 (1.9 Å resolution) reveals that Nb139 binds opposite the DNA-binding surface. Furthermore, we demonstrate that Nb139 does not disturb the functional architecture of the p53 DNA-binding domain using conformation-specific p53 antibody immunoprecipitations, glutaraldehyde crosslinking assays and chromatin immunoprecipitation. Functionally, the binding of Nb139 to p53 allows us to perturb the transactivation of p53 target genes. We propose that reduced recruitment of transcriptional co-activators or modulation of selected post-transcriptional modifications account for these observations.

INTRODUCTION

The p53 protein is of great importance in cancer biology as it mediates innate tumor suppression. This is underscored by its high mutation frequency in human cancers, presence as a germ-line mutation in Li–Fraumeni cancer prone families and highly penetrant cancer predisposition in p53 null mice. Its role as a barrier to tumor development is only one of many as it is centered within numerous signalling pathways. As such, p53 has been widely considered as the master regulator of cell fate in unstressed conditions, where it is held at a basal level by its negative regulator, Mdm2, an E3 ubiquitin ligase, which binds to p53 and targets it for proteasomal degradation. When challenged with various stress conditions, however, this inhibition eases and p53 target genes are transactivated. p53-responsive genes have been documented to be involved in among others cell cycle arrest, apoptosis and senescence (1,2).

Active p53 consists of a tetramer made up of four identical subunits. Each monomer, in turn, retains an architecture commonly found in transcriptional regulators: an N-terminal transactivation domain (residues 1–60), a proline-rich region (residues 63–97), an evolutionarily conserved core DNA-binding domain (DBD) (residues 100–300), a linker region (residues 301–323), a tetramerisation domain (residues 324–355) and finally, a C-terminal regulatory domain (residues 360–393) (3).

p53 is inactivated in over half of all human cancers, either through *TP53* mutations or through alterations in genes encoding up- and downstream regulators of p53. In the former case, over 80% of cancer-derived p53 mutations are found within the DBD (4). This clearly illustrates the importance of the DBD. To date more than 125 protein-coding genes have been documented to be direct transcriptional targets of p53 (5). Aside from being a transcriptional co-activator, p53 is also known for transcriptional repression (6). In ad-

*To whom correspondence should be addressed. Tel: + 32 9 2649340; Fax: + 32 9 2649490; Email: jan.gettemans@ugent.be

dition, it has even been demonstrated that p53 can exercise its influence through a transcription-independent apoptotic response (7).

Multiple mechanisms within the cell are in play to fine-tune the p53 transcriptional program. These include posttranslational modifications of p53, covalent and non-covalent p53 binding partners and p53 response elements of variable binding affinity. Each of these features dynamically adds to the combinatorial regulation of the p53 response, and this magnitude of variables has made understanding the p53 transactivation requirements a formidable task (1,8). A prerequisite therefore is that potent research tools are available. As such, p53 over-expression and knock-out mutations among others have been repeatedly applied to great effect. However, investigating p53 at an endogenous level in a non-invasive manner still remains tasking.

Here, we produced versatile and functional monoclonal single chain antibodies against the p53 DBD based on camelid heavy-chain-only antibodies. These single chain antibodies, also known as nanobodies, represent the smallest (15 kDa), intact, native antigen-binding fragment (9). Their specific biophysical and biochemical properties and their potential of targeting novel epitopes render them a potent research tool in diverse fields, e.g. oncology (10–13), parasitology (14,15), neuropathology (16) and immunology (17).

These nanobodies were applied with great effect within the cell as intrabodies and proved to be an effective research tool to manipulate the p53 transcriptional program. We show that a nanobody is able to disrupt the p53 transcriptional program without altering endogenous p53 levels in a radical fashion.

MATERIALS AND METHODS

Reagents and antibodies

Anti-V5 was purchased from Invitrogen (Merelbeke, Belgium). Anti-p53 (DO1), etoposide, nutlin-3a, RNase A, proteinase K and glutaraldehyde were purchased from Sigma-Aldrich (Diegem, Belgium). Anti-HA was purchased from Roche Applied Science (Vilvoorde, Belgium). Anti-p63 (BC4A4) was purchased from Abcam (Cambridge, UK). Anti-p73 (E4) and anti-NTF2 were purchased from Santa Cruz Biotechnology (Heidelberg, Germany). Anti-βactin (C4) was purchased from MP Biomedicals (Illkirch, France).

Generation of nanobodies

p53 nanobodies, raised against the p53 DBD (residues 92–312), were obtained in collaboration with the VIB Nanobody Service Facility. The immunization and panning procedures, essential for obtaining the p53 nanobodies, were performed as previously described (18). Recombinant V5-tagged nanobodies were generated for immunoprecipitation experiments. The V5-tag allows retrieval of nanobodies using anti-V5 antibody coupled to agarose. Cloning, expression and purification of recombinant V5-tagged nanobodies were performed as previously described (18). The nanobodies were also re-cloned in a modified pcDNA3.1 His_6 vector (Invitrogen) or in the pLVTX Tight Puro vector (Clontech, Saint-Germain-En-Laye, France) for transient intracellular expression or generation of stably expressing cell lines, respectively (see below).

Generation of recombinant untagged p53 DBD

The p53 DBD (residues 92–312) was purified as previously described (19). Briefly, the cDNA fragment was subcloned in the pTYB12 vector (NEB, Evry, France). An initial affinity purification, using chitin resin (NEB), was performed according to the manufacturers' instructions. The purified protein was successively processed via a Superdex 75 (16/60) (GE Healthcare) (150 mM NaCl, 50 mM Tris, 5 mM DTT, pH 8.0) and a HiTrap Heparin column (GE Healthcare) (50 mM NaCl, 20 mM Tris, 5 mM DTT, pH 8.0). The final concentration was determined using a spectrophotometric approach. The p53 DBD was finally dialyzed against 50 mM Tris, 150 mM NaCl, 5 mM DTT, pH 8.0 and stored at −20°C.

Cell culture and transfection

U2OS, U2OS pGL13 and HEK293T cell lines were cultured at 37°C, 10% CO_2 in DMEM (Gibco Life Technologies, Gent, Belgium) supplemented with 10% FBS. Transient transfections were executed with Jetprime (Polyplus Transfections, Illkirch, France) and performed according to the manufacturers' instructions.

Generation of stable U2OS cell lines

U2OS cells stably expressing V5-tagged p53 DBD Nbs or GFP Nb were developed using the Lenti-XTM Tet-OnR Advanced Inducible Expression System from Clontech as previously described (13). Briefly, 250×10^3 cells were seeded in a six-well plate, after which viral mixture (nanobody and regulator) (MOI: 10) was added in a total amount of 2 ml. Cells were then centrifuged for 1 h at 1200 g, after which a two-week selection procedure with neomycin (0.4 mg/ml) and puromycin (1 μg/ml) followed. Expression of nanobodies was induced by the addition of 500 ng/ml doxycycline for 24–48 h.

Immunoprecipitation and immunoblotting

U2OS and/or HEK293T cells were treated with ice-cold lysis buffer (PBS, 0.5% NP-40, 1 mM PMSF and a protease inhibitor cocktail mix) and the extract was centrifuged for 10 min at 20×10^3 g at 4°C. Concentration of the cytoplasmic extract was determined using a Bio-Rad protein assay (Bio-Rad Laboratories, Nazareth Eke, Belgium) according to the manufacturers' prescriptions. Subsequently 0.5 mg of cytoplasmic extract was incubated with 2–5 μg recombinant V5-tagged nanobody or 2–5 μg lgG antibody of interest for 1–2 h at 4°C. The former step was skipped when working with stable nanobody-expressing U2OS cell lines. Afterward, 15 μl anti-V5 agarose (Sigma) or proteinG sepharose (GE Healthcare) was added to the sample and incubated for 1–2 h at 4°C. The beads were washed with lysis buffer, boiled for 5 min in Laemmli sample buffer and proteins were fractionated by sodium dodecyl sulphate-polyacrylamide gel electrophoresis (SDS-PAGE). Western blotting was performed as previously described (20).

Isothermal titration calorimetry

The binding affinity of p53 DBD to p53 DBD Nb139 was measured at 30°C by isothermal titration calorimetry (ITC) using a Microcal VP-ITC as previously described (18). Untagged p53 DBD and V5-tagged p53 Nb139 were dialyzed against 20 mM Tris, 150 mM NaCl, pH 7.5. The precise protein concentrations used for the ITC are described in Supplementary Figure S1. ITC data was fitted using a 'One Set of Sites' model.

Luciferase assay

A luciferase assay was performed as previously described (21). Briefly, 180 × 10^3 U2OS cells in which the pGL13 luciferase reporter is stably integrated were plated on 12-well plates 1 day before transfection. A nanobody and a beta-galactosidase vector were co-transfected (see above). At 24 h post-transfection, the cells were reseeded in a 96-well plate and treated with or without nutlin-3a (5 μM). The next day, luciferase activity from triplicate samples was measured by chemiluminescence with a Topcount luminometer (Canberra-Packard). The level of firefly luciferase activity was normalized by that of the beta-galactosidase activity in each experiment.

Real-time quantitative PCR

Total RNA was isolated from a stable nanobody-expressing U2OS cell line using a High Pure RNA Isolation Kit (Roche) according to the manufacturers' preferences. RNA quality was assessed for each sample by determining the 260/280 ratio using a spectrophotometer (Nanodrop, Wilmington, DE, USA). Complementary DNA (cDNA) was immediately synthesized using a Transcriptor First Strand cDNA Synthesis Kit with oligo(dT) primers (Roche). The cDNA concentration was determined using a spectrophotometer. Samples were stored afterward at −80°C.

Primers for *PUMA*, *GADD45a* and the reference genes (*ACTB*, *B2M*, *GADPH*, *G6PDH*, *PGK1* and *cyclophilin*) were in-house validated. All primer efficiencies lie within the range of 90–110%. The sequence of the primers can be found in Supplementary Table S1. Primers for *p21* (#631) and *MDM2* (#3499) were derived from RTPrimerDB (22).

RTqPCR was performed using a LightCycler 480 (96-plate platform) (Roche). Each reaction consisted of 6 μl of cDNA (1/12 dilution) mixed with 0.75 μl of a 10 μM solution of each primer and 7.5 μl of 2× LC480 SYBR Green Master (Roche). The PCR conditions were as follows: 10 min at 95°C, followed by 45 cycles of denaturation (10 s at 95°C), and elongation (45 s at 60°C). All reactions were performed in triplicate and no template controls were included for all genes.

Stability analysis of the different references was performed using the geNormPLUS application in the qbasePLUS software version 2.0 (Biogazelle, Zwijnaarde, Belgium) (23).

Crystallization and structure determination

Nb139 and p53DBD, both dialyzed against 50 mM NaCl, 50 mM Tris, 5 mM DTT, pH 7.2, were mixed at a 1.2:1 ratio to a final concentration of 6.56 mg/ml, before adding the freshly formed complex to the crystallization set-up. After screening with commercially available crystallization kits, crystals of the complex were obtained at 20°C using the hanging-drop vapor diffusion method (24) after mixing 1 μl protein solution with 1 μl reservoir solution equilibrated against 125 μl 0.2 M potassium formate 20% w/v PEG 3350 reservoir solution (Molecular Dimensions JCSG+ condition 1.10). The crystals were cryoprotected by transfer to a solution consisting of 0.2 M potassium formate 20% w/v PEG 3350 and 20% glycerol and subsequently vitrified in liquid nitrogen. Data was collected at 100 K on the Proxima1 beamline of the SOLEIL synchrotron on a 6M Pilatus detector (Gif-Sur-Yvette, France). One Nb139/p53 core domain co-crystal diffracted to 1.9 Å resolution and a full data-set was collected. The crystal belongs to space group $P2_12_12_1$ with unit-cell dimensions $a = 46.4$ Å, $b = 68.3$ Å and $c = 110.0$ Å.

Data was processed with the software package *XDS* (25) and the unit-cell content was estimated with the program *MATTHEW_COEF* from the CCP4 program suite (26). A molecular replacement approach was applied with PHASER-MR (27) using a search model with the coordinates of the a nanobody against *Escherichia coli* MazE (PDB entry 1MVF). Prior to the search all three complementarity determining regions were deleted. Using the molecular replacement solution, ARP/wARP (28) rebuilt the correct model to almost completion. The refinement was completed by combining manual building using Coot (29) and automated maximum likelihood refinement as implemented in *phenix.refine* (30). Structure quality was checked using the MolProbity (31). Full data collection and refinement statistics are reported in Supplementary Table S2. The extreme 21 C-terminal p53DBD residues were missing and were thus not included in subsequent analysis. Surface accessibility was determined with Nacces 2.1.1 using a probe with a radius 1.4 Å (32), and residues involved in hydrogen bond formation and van der Waals interactions were determined by HBPLUS v.3.06 (33) and as residues harboring non-hydrogen atoms in their environment closer than 4 Å, respectively. These data are reported in Supplementary Table S3.

Crosslinking assay

HEK293T cells were transiently transfected with indicated nanobody plasmids and lysed with lysis buffer (0.5% NP-40, 50 mM Tris-HCl pH 7.5, 150 mM NaCl, 50 mM NaF, 1 mM NaVO3, 1 mM DTT, 1 mM PMSF and protease inhibitor mixture) 36 h after transfection. Glutaraldehyde was added to the lysate at indicated concentrations. After incubating the lysate on ice for 20 min, the glutaraldehyde reactions were stopped by adding Laemmli sample buffer, and the samples were heated at 100°C for 5 min and resolved by SDS-PAGE. Western blot analysis was performed with anti-p53 antibody (DO1).

Chromatin immunoprecipitation

A chromatin immunoprecipitation (ChIP) assay was performed as previously described (34). Briefly, lysates from

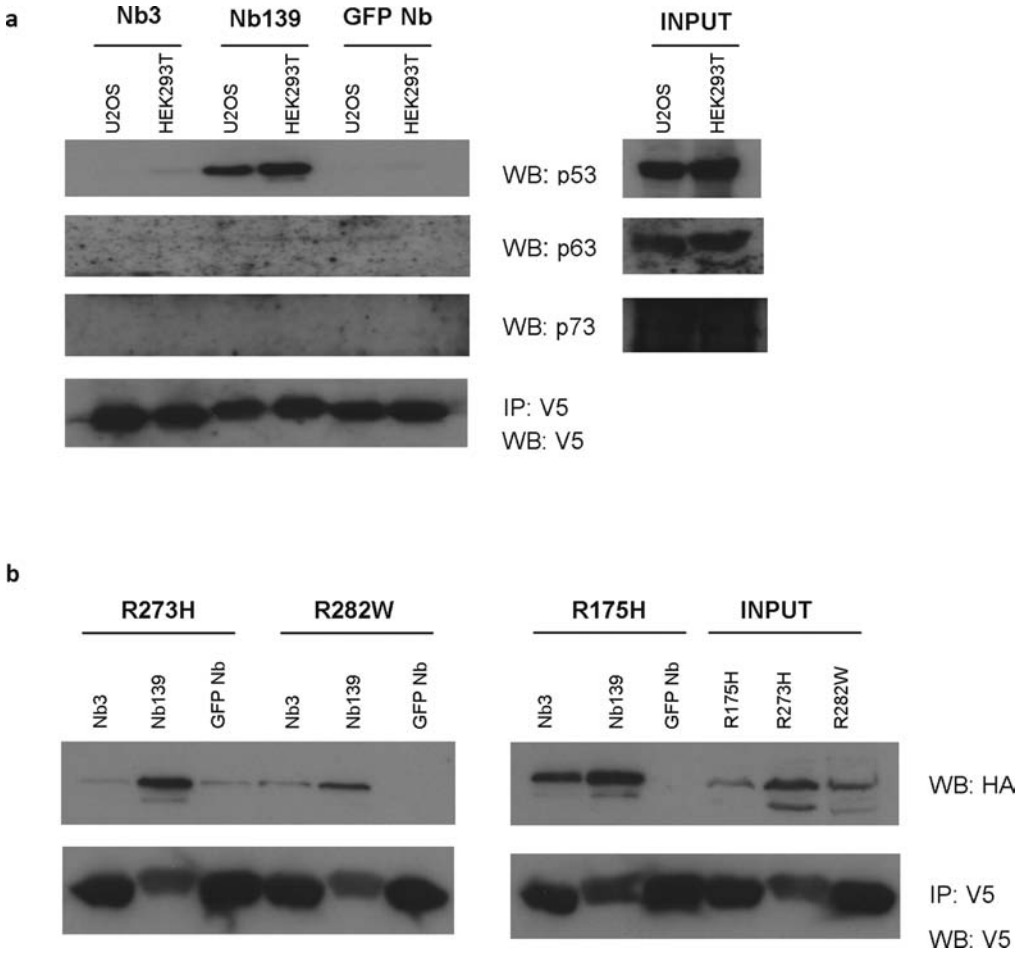

Figure 1. Characterization of p53 DBD Nanobodies. (**a**) Recombinant V5-tagged Nb3, Nb139 or GFP Nb (2 μg) were added to *wild type* p53-bearing U2OS and HEK293T cell lysates (500 μg). Nanobody–protein complexes were immunoprecipitated and analysed for the interaction with p53 protein family members. Nb139 is only able to interact with *wild type* p53, leaving p63 and p73 unaffected. (**b**) Recombinant V5-tagged nanobodies (2 μg) were added to HEK293T cell lysates (500 μg), in which HA-tagged *hot spot* p53 mutants, i.e. R175H, R273H and R282W, were expressed at variable levels (see input). A co-immunoprecipitation was performed relying on the V5-tagged nanobodies. The mutual interaction between mutant p53 and nanobody was subsequently analysed via western blot. Nb3 has a preference for 'structural' mutant p53, i.e. R175H and R282W, while Nb139 binds p53 irrespective of the mutation. The binding characteristics of Nb3 and Nb139 are compared to that of the control GFP Nb.

stable nanobody-expressing U2OS cell lines were sonicated with a Bioruptor Sonication System UCD-300 (Diagenode, Seraign, Belgium) 21 times for 30 s with intermittent cooling. Anti-p53 (DO1) was used to perform the precipitation of the DNA-bound p53, whereas anti-NTF2 was used as an aspecific control. The chromatin-antibody protein complex was eluted from the protein-G-Sepharose beads with freshly prepared elution buffer (0.1 M NaHCO3 and 1% SDS). Reverse crosslinking and RNase treatment of the ChIP eluate were simultaneously performed overnight at 65°C. The samples were digested with proteinase K for 3 h at 50°C. The DNA was finally purified using QIAquick PCR Purification Kit (Qiagen, Venlo, The Netherlands). The eluted DNA was subsequently submitted to a RTqPCR (see above). The sequences of the primers used can be found in Supplementary Table S4 (35).

RESULTS

Nanobody 3 and nanobody 139 target the p53 DBD

We developed two single domain antibodies against the DBD of p53, termed Nb3 and Nb139 (see Materials and Methods). Their binding specificity was determined by investigating the cross-reactivity with members of the p53 protein family, i.e. p53, p63 and p73. The p53 family members retain a similar basic modular structure. However, despite a rather limited overall homology, they display 60% similarity within the DBD (36). By using a co-immunoprecipitation set-up we incubated recombinant Nb3, Nb139 or a control GFP Nb (37) with either HEK293T or U2OS cell lysates. In both cases, Nb139 was able to bind endogenous *wild type* p53 but did not interact with p63 nor with p73 (Figure 1a). Nb3 on the other hand failed to show a significant interaction with *wild type* p53 or with the other p53 protein family members. Interestingly, in over-expression experiments using HA-tagged *hot spot* p53 mutants, we observed that Nb3 preferentially inter-

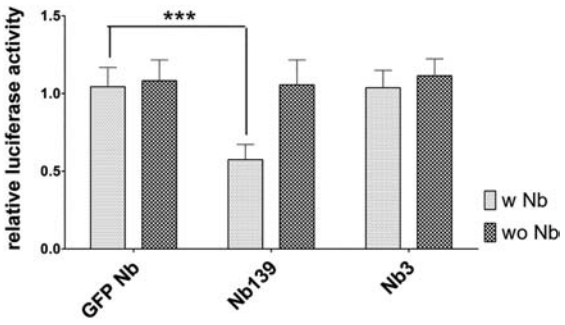

Figure 2. Establishment of Nb139's inhibitory effect on the p53 transcriptional program. The relative luciferase activity was measured in U2OS cells stably harboring a luciferase gene. This cell line was transiently transfected with (w) or without (wo) Nb3, Nb139 or GFP Nb, and treated 24 h post-transfection with nutlin-3a (5 μM) for an additional 24 h. The luciferase activity was then finally measured. Nb139 causes a significant reduction in luciferase transcription in comparison to the control GFP Nb. An unpaired student t-test was performed (*** < 0.001).

acted with 'structural' mutant p53, i.e. R175H and R282W (Figure 1b), in comparison to the control GFP Nb. Nb139, on the other hand, interacted with p53, regardless of mutations in the DBD. These 'structural' mutants are known to destabilize the overall architecture of the DNA-binding surface, rendering the p53 protein inactive (3). As a result, it was not opportune to evaluate the effect of Nb3 on the transcriptional characteristics of *wild type* p53, in contrast to Nb139. Nb3 was therefore included, in addition to the GFP Nb, as a control in subsequent experiments.

The K_D of Nb139 determined by ITC is ∼1 μM (Supplementary Figure S1a and b). This rather weak K_D indicates that the interaction between the p53DBD and Nb139 is of a transient nature. However, depending on the molecular environment, volatile protein–protein interactions are known to change their characteristics and obtain a more permanent binding pattern (38,39). The binding affinity value is thus merely to be considered indicative for a cellular context. In addition, the binding stoichiometry with which Nb139 interacts with the p53DBD was determined at 1:1. Thus, since Nb139 conformed to the needs for a precise research tool, i.e. specificity and affinity, we set out to investigate the influence of Nb139 on the transcriptional program of *wild type* p53.

Nb139 perturbs the p53 transcriptional program in a non-specific fashion

With Nb139 specifically targeting the *wild type* p53DBD, we assessed how it would alter the transcriptional functions attributed to this domain. Therefore, we performed a transactivation assay by transiently transfecting Nb3, Nb139 or the control GFP Nb in U2OS cells stably harboring a luciferase reporter gene. The luciferase cDNA is preceded by 13 repeats of a p53 consensus response element. We found that Nb139 is able to significantly diminish luciferase expression in comparison to the control condition (Figure 2). Thus, it became apparent that Nb139 can influence the p53 transcriptional program. We took this one step further by looking into the regulation of p53 target genes.

To succeed in this endeavor we developed U2OS cell lines with doycycline-inducible nanobody expression. This not only guarantees a homogenous nanobody expression throughout the cell population but also allows us to tune nanobody expression (Figure 3a). p53 isoform specificity is corroborated in these cell lines (Supplementary Figure S2).

Next, we performed a RTqPCR, establishing that Nb139 suppresses p53's transcriptional program. The mRNA levels of p53 target genes involved in cell cycle arrest (i.e. *p21*, *GADD45A*), apoptosis (i.e. *PUMA*) and p53 regulation (i.e. *MDM2*) all decreased in a significant manner in the presence of Nb139 (Figure 3b). Hence, this nanobody impacts transcription-dependent functions of p53 in a non-specific fashion.

The structural evidence advocates a rupture of the functional architecture of p53

To understand at the molecular level how Nb139 quenches the p53 transcriptional program, we determined the co-crystal structure of the p53DBD in complex with Nb139. The structure was obtained at a resolution of 1.9 Å and reveals that Nb139 binds the immunoglobulin-like β-sandwich fold of the DBD on the opposite side of the DNA-binding surface (Figure 4a). While four other crystal packing contacts between Nb139 and the p53DBD could be identified, none of them made extensive protein–protein interactions through the complementary determining regions (CDRs) of the nanobody (Supplementary Table S3). The DBD consists of a hydrophobic core formed by the stacking of two twisted antiparallel β-sheets. This inner core is flanked by the DNA interaction surface, which involves two loops stabilized by a zinc ion, and a loop-sheet-helix motif. On the opposite side of the DBD, the three CDRs of Nb139 enclose the leucine-rich loop connecting β-strand 9 and β-strand 10, thereby anchoring CDR2 into the core of the β-sandwich through the formation of hydrogen bonds and van der Waals interactions (Figure 4a and Supplementary Table S3). The backbone of residues Gly104 and Pro101 of CDR3 form hydrogen bonds with the side chains of Ser261 and Asn263 respectively while residues Thr32 of CDR1 and Trp54 of CDR2 form backbone–backbone hydrogen bonds with Gly262 and Leu264 of the p53 core domain (Figure 4b).

We performed a backbone superposition of 194 atoms (Ser96 to Leu264) of the DBD from the Nb139/DBD complex with four molecules of the asymmetric unit from the previously determined free human DBD (PDB entry 2OCJ (40)). This resulted in RMSDS of 0.54, 0.53, 0.51 and 0.67 Å respectively. Overall, the structure distinctively illustrated that Nb139 does not disturb the architecture of the DBD. To corroborate this finding, we performed a co-immunoprecipitation using conformation-specific p53 antibodies Ab1620 (*wild type*) and Ab240 (mutant) (Figure 4c) (41). To this end, recombinant Nb3, Nb139 or the control GFP Nb were incubated with either HEK293T or U2OS cell lysates, after which the conformation-specific antibodies were added in order to bind either *wild type* or mutant p53. In the presence of Nb139, Ab1620 was still able to interact with p53 suggesting that p53's functional architecture remains intact. However, the co-immunoprecipitation

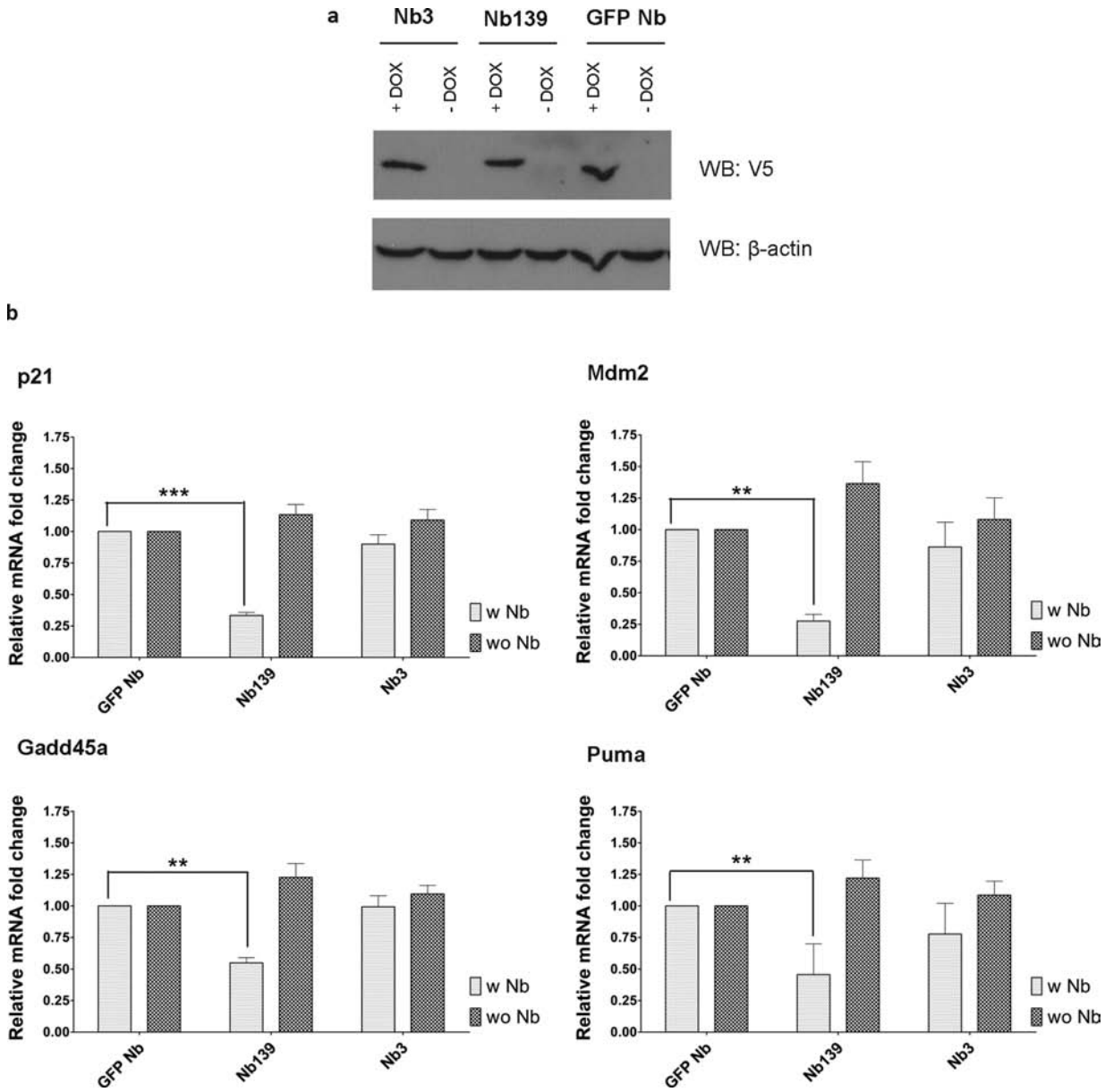

Figure 3. Nb139 reduces transcription of various p53 target genes. (**a**) Inducible expression of V5-tagged nanobodies in U2OS cells was verified in the absence (−DOX) or presence (+DOX) of 500 ng/ml doxycycline (50 μg crude lysate was loaded). (**b**) U2OS cell lines were consecutively treated with doxycycline (500 ng/ml) (24 h) and etoposide (20 μM) (24 h), after which the transcription levels of p53 target genes (*p21*, *MDM2*, *GADD45a* and *PUMA*) were evaluated via RTqPCR. Irrespective of the target gene, Nb139 is able to significantly reduce mRNA levels in comparison to control conditions. A paired student t-test was performed (** < 0.01 and *** < 0.001).

experiment also revealed that, in comparison to the other conditions, Nb139 is only slightly more present in the p53-Ab1620 complex. Thus, Nb139 could possibly not adequately bind p53 in the presence of Ab1620. In addition, minor structural variations are present at the interaction interface as the turn between β-strand 9 and β-strand 10 is displaced away from the inner core of the p53 β-sandwich upon binding of Nb139 (Figure 4d). As follows, we are strongly inclined to conclude that Nb139 leaves the DBD's architecture unaffected, but additional experimentation is needed to confirm this with absolute certainty.

Recently, the structure of a tetrameric DBD bound to the full consensus site was solved, revealing a co-operative self-assembling process for oligomerization (PDB entry 3KMD (42)). First, two DBD monomers (A and B) form a p53 dimer across one half site of the DNA by making distinctive protein–protein and protein–DNA interactions (Figure 5). Subsequently, identical dimers can bind the dimeric complex. In this configuration, each DBD monomer is stabilized through protein–protein interactions at the dimer and dimer–dimer interface as well as through protein–DNA interactions, resulting in a stable tetrameric complex. This oligomerization process is mediated through essential con-

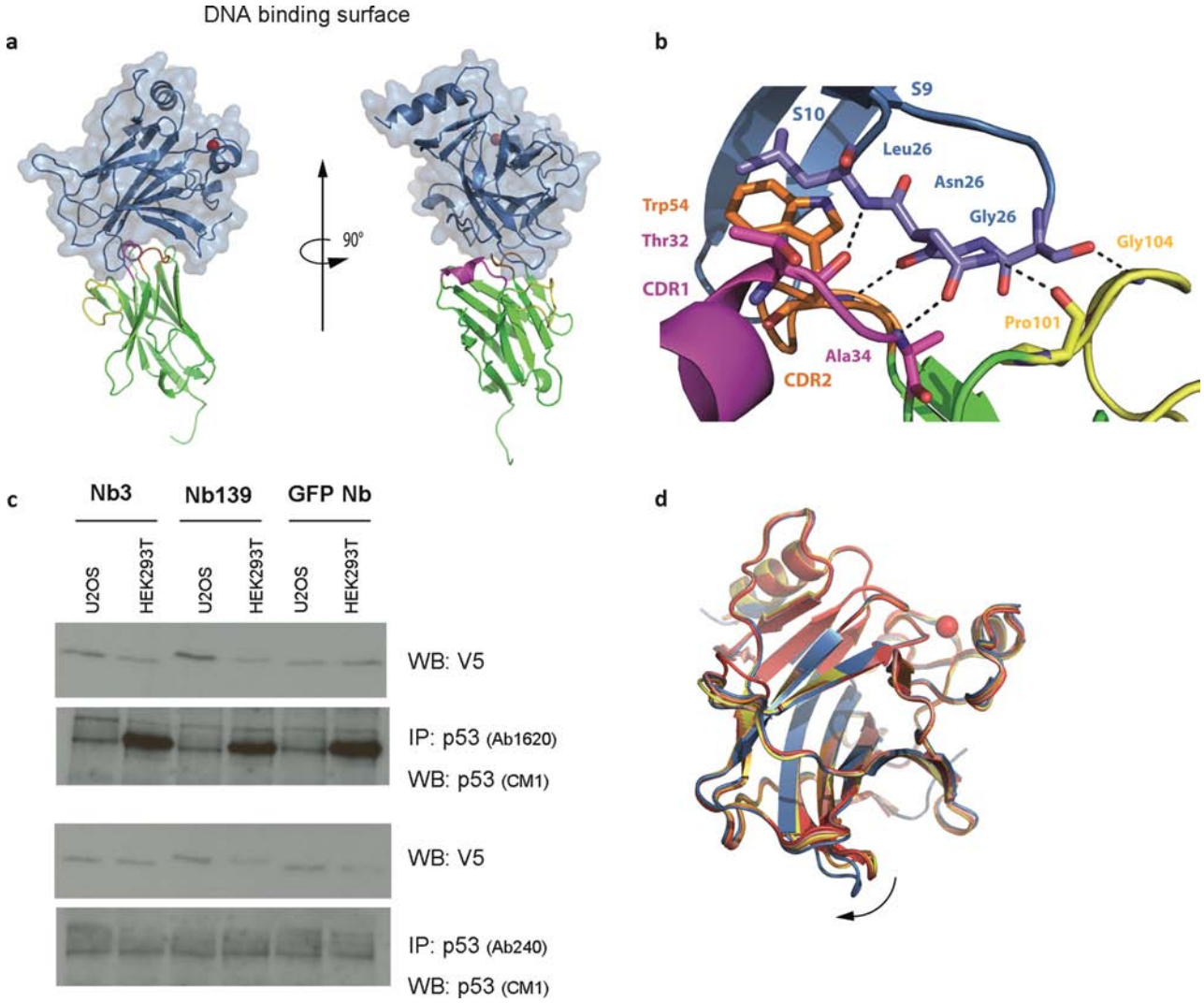

Figure 4. Structure of the Nb139/DBD complex. (**a**) Nb139 (green) with CDR1 (magenta), CDR2 (orange) and CDR3 (yellow) represented in cartoon, bound to p53 core domain (blue) represented in cartoon/surface. The zinc ion of the DNA-binding interface is represented as a red sphere. (**b**) The interaction between Nb139 and the DBD is established by hydrogen bounds (dashed lines) between the backbone and side chains of CDR1, CDR2 and CDR3 with the leucine-rich loop connecting the β-strand 9 and β-strand 10 of the p53 core domain. (**c**) U2OS or HEK293T cell lysate (500 μg) were successively incubated with recombinant V5-tagged Nb3, Nb139 or GFP Nb (2 μg) and 5 μg of p53 conformation-specific antibodies, i.e. Ab1620 (*wild type*) or Ab240 (mutant). Nanobody-p53 complexes were immunoprecipitated (relying on the used conformation-specific antibodies) and analysed for the presence of p53. Nb139, nor other nanobodies, influences the architecture of p53. In addition, the presence of p53-bound nanobody was also evaluated via western blot. (**d**) Backbone superposition of the p53DBD of the Nb139/DBD (blue) and four molecules of the asymmetric unit of 2OCJ (red, orange, yellow and pink). Upon binding of Nb139, the loop connecting β-strand 9 and β-strand 10 is displaced away from the inner core of the β-sandwich fold (arrow).

formational changes in the backbone and side chains of residues of the DBD at the dimer–dimer interface, resulting in tight surface complementarity (42).

Although the p53 dimer on its own is symmetrical (in regard to the position of Nb139), formation of the dimer–dimer complex breaks the symmetry. The result is two unique binding sites for Nb139 when encountering a tetrameric complex. The first one is located on the outer side of the B and D core domain (Figure 5, green Nb139) while the second one is located at the dimer–dimer interface (Figure 5, orange Nb139). In the latter possibility, the positively charged side chain of Arg28 of Nb139 would coincide with side chains of Val225 and Lys101 at the patch II thereby breaking the dimer–dimer interface. Unfortunately, electron density for Arg28 of CDR1 was lacking in the Nb139/p53DBD domain complex, indicating disorder, and could not be represented on the superposition. However, this superposition suggests that Nb139 might prevent the formation of the tetrameric complex but not the p53 core domain dimer.

Nb139 permits endogenous p53 to bind p53-responsive promoters

To validate the hypothesis that Nb139 interferes with tetramer formation, we performed a crosslinking assay by treating transiently nanobody-transfected HEK293T cells

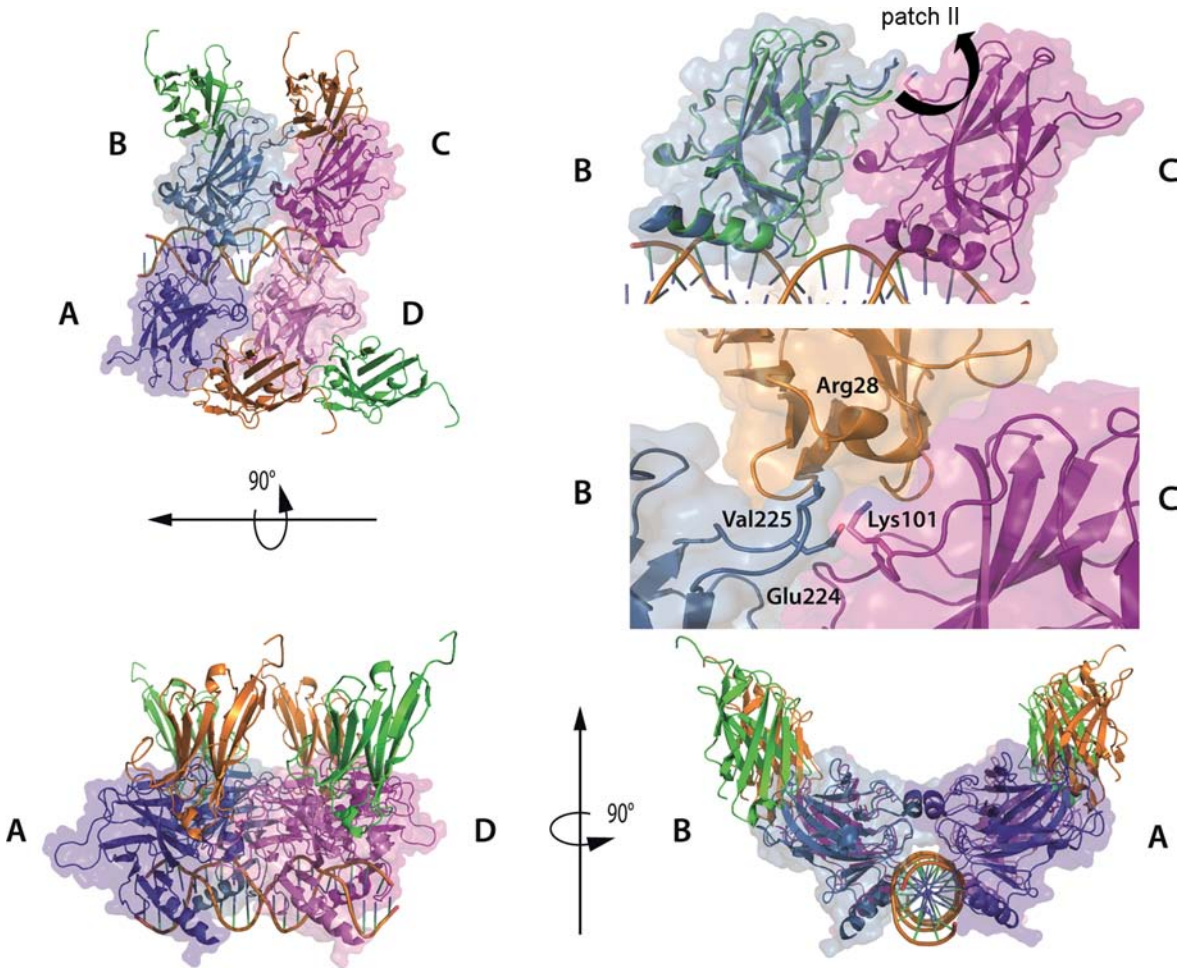

Figure 5. Superposition of Nb139 onto the tetrameric DBD in complex with its consensus site. Top and side views of the superposition of Nb139 onto the p53 dimer (AB, blue)–dimer (CD, pink) of 3KMD reveals two possible binding sites. The green Nb139 is positioned outward on the tetramer while the orange Nb139 is positioned at the side of the dimer–dimer interface. Binding at patch II of the dimer–dimer interface induces conformational changes in loop β7–β8 away from the p53 DBD monomer position (green). Binding of Nb139 might prevent tetramerization by disrupting the formation of patch II with Arg28 of CDR1. Electron density of the Arg28 side chain was lacking, indicating disorder.

with increasing amounts of glutaraldehyde. This set-up demonstrated elegantly that Nb139 still allows the formation of p53 di- and tetramers (Figure 6a), both of which form the basis for p53's functional transcriptional characteristics. As to see if this also meant that p53 is still able to functionally bind its response elements *in vivo*, we executed a ChIP assay by using a commercial p53 antibody (DO1) to precipitate a p53/chromatin-complex. Hereby, we found strong indications that Nb139 preserves the DNA-binding characteristics of p53, with p53 binding the response elements of *p21* and *MDM2* (Figure 6b). Thus, another transcriptional inhibitory mechanism, e.g. the reduced recruitment of transcriptional co-activators, must be at play as Nb139 is able to modulate the p53 transcriptional program while leaving the p53 conformation unaffected.

DISCUSSION

The p53 protein is indisputably an important tumor suppressor and is often referred to as 'the guardian of the genome' (43). In unstressed conditions p53 is held at basal levels, while a wide variety of intra- and extracellular stress signals promote p53 stabilization and activation. As such, p53 is able to provide an appropriate transcription-dependent and -independent response, contributing to diverse biological functions, e.g. cell cycle arrest, apoptosis, angiogenesis, energy metabolism, motility and migration (44). We are at the beginning of understanding many of these functions and the mechanism by which p53 is regulated. It is clear, for example, that p53 transcriptionally regulates the expression of different genes. The p53 transcriptional program is fine-tuned by many mechanisms, which enable p53 to differentiate between the vast repertoire of target genes (8,45). Among others, post-translational modifications of p53, (non)covalent p53 binding partners and p53 response elements of variable binding affinity. However, despite intensive effort, this area of study still remains elusive.

Technological innovations have always proven to advance the knowledge of p53. The development of p53 genotype-specific knock-in/out mice (46), conformation-specific antibodies (41), p53-null cell lines (47), p53-specific siRNA (48), MDM2 inhibitors (49) and many more have all contributed

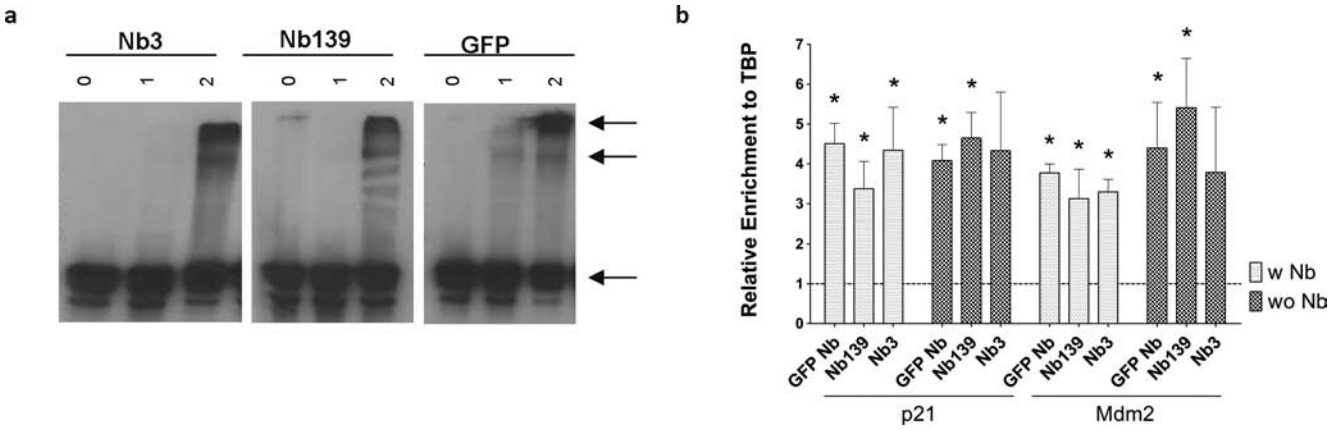

Figure 6. Nb139 maintains *wild type* conformation of p53. (**a**) The p53 monomers, derived from transiently nanobody-transfected HEK293T lysates, were crosslinked with an increasing amount of glutaraldehyde (0: 0%, 1: 0.001% and 2: 0.01%). All three nanobody conditions allow p53 to form dimers and tetramers. Arrows indicate mono-, di- and tetramer conformation of p53. (**b**) The U2OS cell lines were consecutively treated with doxycycline (500 ng/ml) (24 h) and etoposide (20 μM) (24 h), after which the ChIP was performed. In the presence of Nb139 p53 is able to bind *in vivo* the response elements of *p21* (primer set F) and *MDM2* (primer set E). After taking the background signal (i.e. signal derived from the input and anti-NTF2 antibody control) into account, Nb139 differs in a similar significant fashion as GFP Nb from the reference *TBP* gene. A paired student t-test was performed (* < 0.05). In the absence of Nb3, p53 binds to p21 and MDM2, but not in a significant manner with *P*-values of respectively 0.059 and 0.063.

pieces to the ever-growing complex p53 puzzle. However, past studies have revealed a disparity between several hypotheses generated by *in vitro* transfection studies and *in vivo* mouse models, which is probably explained by the ability of mouse models to preserve crucial stoichiometric relationships between p53 and its negative and positive regulators (50). Nevertheless, *in vitro* studies will remain indispensable as they provide a cost/time-effective, important source of scientific data, that in turn can be validated *in vivo*.

Taking both of these concerns into consideration, we have applied nanobody technology to the field of p53. We have developed research tools, Nb3 and Nb139, which allow us to specifically target endogenous p53 in a non-invasive manner. Nb3 binds 'structural' mutant p53. Despite us not having investigated its full potential, Nb3 may be of invaluable importance in the field of re-activating loss-of-function p53 (51,52). Liu *et al.* recently proposed certain criteria to screen for genuine p53 re-activation (53). With Nb3 already complying with one of these criteria, i.e. the specific binding of 'structural' mutant p53, Nb3 is potentially considered a valid candidate. If further research confirms that Nb3 revives mutant p53, this nanobody could accelerate the rational design of small molecules capable of stabilizing mutant p53. As small molecule drug design is supported by structural biology, the co-crystal structure of Nb3 in complex with the DBD could help identify the crucial binding site or help generate hypotheses for structure-based design for new p53 re-activating compounds (54).

Nb139, on the other hand, targets both mutant and *wild type* p53. Specifically focusing on *wild type* p53, we demonstrate that Nb139 is able to inhibit the transcriptional capabilities of p53 with surgical precision, as it maintains the functional architecture and the DNA-binding characteristics of p53. However, as to exclude possible ambiguousness, regarding Nb139's traits, additional experimentation can be of interest. Assays such as circular dichroism, an electrophoretic mobility shift assay or a Nb-based ChIP assay, could unequivocally corroborate our findings that point toward the conservation of the functional architecture of p53 in the presence of Nb139.

Other existing research tools fail to specifically target single functions of p53. For example, pifithrin-α (55) does not only exploit the p53 pathway but also heat shock and glucocorticoid receptor signalling, among others (56,57). By manipulating the p53 pathway in such a gentle manner, Nb139 creates a unique opportunity to investigate the combinatorial effects of, e.g. p53 binding proteins, post-translational modifications and stress signals on the transcriptional program. Since the p53 response is context-dependent, and we only tested U2OS cells treated with etoposide, the application of Nb139 in various backgrounds, with regard to use of cell lines and stress-inducing treatments, will undoubtedly provide insight into the regulatory mechanics of the transcription-dependent functions.

Additionally, Nb139 may be of interest in regard to the transcription-independent functions of p53 as the DBD is also an instrument of apoptotic regulation in the cytosol (7,58,59). Mihara *et al.* first touched upon the subject of transcription-independent functions of p53 (7). Since then, this process has been well characterized (60). However, certain questions do remain, e.g. interaction of p53 with Bcl2 protein family members and the effect(s) of mutant p53 in the cytosol. As such, Nb139 may prove to be an ideal crystallization chaperone (61) to stabilize the weak p53-BAX interaction, since it theoretically does not interfere with the p53-protein-binding interface. This would thus allow to elucidate the molecular details of this interaction.

Furthermore, both nanobodies can also be applied to track the localization of cytosolic mutant p53 as it has not been established whether mutations in p53 affect its cytoplasmic translocation (62). The application of nanobodies as intracellular probes has already been demonstrated in numerous cases (10,11,13,16,17,63). In addition, Nb139 can be used as a stepping stone for the rational design of gain-of-function inhibitors. As most common types of cancer-associated p53 mutations abrogate p53's tumor suppressive

activity, it has also been established that some endow the mutant protein with new activities, e.g. enhanced invasion and anti-apoptotic activity, that actively contribute to various stages of tumor progression and increase resistance to anticancer treatments (64). As such, mutant p53 is a valid target for inactivation by prospective anticancer therapies.

In conclusion, Nb3 and Nb139 are novel research tools that will permit an innovative approach to various branches of the intricate field of p53.

SUPPLEMENTARY DATA

Supplementary Data are available at NAR Online.

ACKNOWLEDGEMENT

I would like to thank the following people for invigorating discussions that have been paramount to the shaping of this scientific work. Prof. Dr Jean-Christophe Marine (VIB-KULeuven), Dr Rainer Wilcken (Novartis Institutes), IR. Anneleen Vuchelen (VIB-VUB), Wouter Van Overbeke (Nanobody Lab) and Dr Davina Tondeleir (King's College London). The U2OS pGL13 cell line was a kind gift from Prof. Dr Joost Schymkowitz and Prof. Dr Frederic Rousseau (VIB-KULeuven).

FUNDING

Agency for Innovation by Science and Technology in Flanders (IWT-Vlaanderen; to J.B.); League against Cancer (Stichting tegen Kanker, Belgium) [202-2008]; Ghent University (BOF-GOA) [BOF13/GOA/010]; the Research Foundation-Flanders (FWO-Vlaanderen) [G.0223.10N]; Interuniversity Attraction Poles program (IUAP) [P7/13]. Funding for open access charge: Interuniversity Attraction Poles program (IUAP) [P7/13].
Conflict of interest statement. None declared.

REFERENCES

1. Bieging,K.T. and Attardi,L.D. (2012) Deconstructing p53 transcriptional networks in tumor suppression. *Trends Cell Biol.*, **22**, 97–106.
2. Vousden,K.H. and Lu,X. (2002) Live or let die: the cell's response to p53. *Nat. Rev. Cancer*, **2**, 594–604.
3. Joerger,A.C. and Fersht,A.R. (2008) Structural biology of the tumor suppressor p53. *Annu. Rev. Biochem.*, **77**, 557–582.
4. Hainaut,P., Hernandez,T., Robinson,A., Rodriguez-Tome,P., Flores,T., Hollstein,M., Harris,C.C. and Montesano,R. (1998) IARC Database of p53 gene mutations in human tumors and cell lines: updated compilation, revised formats and new visualisation tools. *Nucleic Acids Res.*, **26**, 205–213.
5. Riley,T., Sontag,E., Chen,P. and Levine,A. (2008) Transcriptional control of human p53-regulated genes. *Nat. Rev. Mol. Cell Biol.*, **9**, 402–412.
6. Ho,J. and Benchimol,S. (2003) Transcriptional repression mediated by the p53 tumour suppressor. *Cell Death Differ.*, **10**, 404–408.
7. Mihara,M., Erster,S., Zaika,A., Petrenko,O., Chittenden,T., Pancoska,P. and Moll,U.M. (2003) p53 has a direct apoptogenic role at the mitochondria. *Mol. Cell*, **11**, 577–590.
8. Beckerman,R. and Prives,C. (2010) Transcriptional regulation by p53. *Cold Spring Harb. Perspect. Biol.*, **2**, a000935.
9. Hamers-Casterman,C., Atarhouch,T., Muyldermans,S., Robinson,G., Hamers,C., Songa,E.B., Bendahman,N. and Hamers,R. (1993) Naturally occurring antibodies devoid of light chains. *Nature*, **363**, 446–448.
10. De Clercq,S., Boucherie,C., Vandekerckhove,J., Gettemans,J. and Guillabert,A. (2013) L-plastin nanobodies perturb matrix degradation, podosome formation, stability and lifetime in THP-1 macrophages. *PloS One*, **8**, e78108.
11. Van Audenhove,I., Boucherie,C., Pieters,L., Zwaenepoel,O., Vanloo,B., Martens,E., Verbrugge,C., Hassanzadeh-Ghassabeh,G., Vandekerckhove,J., Cornelissen,M. *et al.* (2014) Stratifying fascin and cortactin function in invadopodium formation using inhibitory nanobodies and targeted subcellular delocalization. *FASEB J.*, **28**, 1805–1818.
12. Pruszynski,M., Koumarianou,E., Vaidyanathan,G., Revets,H., Devoogdt,N., Lahoutte,T. and Zalutsky,M.R. (2013) Targeting breast carcinoma with radioiodinated anti-HER2 Nanobody. *Nucl. Med. Biol.*, **40**, 52–59.
13. Van Impe,K., Bethuyne,J., Cool,S., Impens,F., Ruano-Gallego,D., De Wever,O., Vanloo,B., Van Troys,M., Lambein,K., Boucherie,C. *et al.* (2013) A nanobody targeting the F-actin capping protein CapG restrains breast cancer metastasis. *Breast Cancer Res.*, **15**, R116.
14. Baral,T.N., Magez,S., Stijlemans,B., Conrath,K., Vanhollebeke,B., Pays,E., Muyldermans,S. and De Baetselier,P. (2006) Experimental therapy of African trypanosomiasis with a nanobody-conjugated human trypanolytic factor. *Nat. Med.*, **12**, 580–584.
15. Ditlev,S.B., Florea,R., Nielsen,M.A., Theander,T.G., Magez,S., Boeuf,P. and Salanti,A. (2014) Utilizing nanobody technology to target non-immunodominant domains of VAR2CSA. *PloS One*, **9**, e84981.
16. VanOverbeke,W., Verhelle,A., Everaert,I., Zwaenepoel,O., Vandekerckhove,J., Cuvelier,C., Derave,W. and Gettemans,J. (2014) Chaperone nanobodies protect gelsolin against MT1-MMP degradation and alleviate amyloid burden in the gelsolin amyloidosis mouse model. *Mol. Ther.*, **22**, 1768–1778.
17. De Clercq,S., Zwaenepoel,O., Martens,E., Vandekerckhove,J., Guillabert,A. and Gettemans,J. (2013) Nanobody-induced perturbation of LFA-1/L-plastin phosphorylation impairs MTOC docking, immune synapse formation and T cell activation. *Cell. Mol. Life Sci.*, **70**, 909–922.
18. Van den Abbeele,A., De Clercq,S., De Ganck,A., De Corte,V., Van Loo,B., Soror,S.H., Srinivasan,V., Steyaert,J., Vandekerckhove,J. and Gettemans,J. (2010) A llama-derived gelsolin single-domain antibody blocks gelsolin-G-actin interaction. *Cell. Mol. Life Sci.*, **67**, 1519–1535.
19. Bullock,A.N., Henckel,J., DeDecker,B.S., Johnson,C.M., Nikolova,P.V., Proctor,M.R., Lane,D.P. and Fersht,A.R. (1997) Thermodynamic stability of wild-type and mutant p53 core domain. *Proc. Natl Acad. Sci. U.S.A.*, **94**, 14338–14342.
20. Towbin,H., Staehelin,T. and Gordon,J. (1979) Electrophoretic transfer of proteins from polyacrylamide gels to nitrocellulose sheets: procedure and some applications. *Proc. Natl Acad. Sci. U.S.A.*, **76**, 4350–4354.
21. Xu,J., Reumers,J., Couceiro,J.R., De Smet,F., Gallardo,R., Rudyak,S., Cornelis,A., Rozenski,J., Zwolinska,A., Marine,J.C. *et al.* (2011) Gain of function of mutant p53 by coaggregation with multiple tumor suppressors. *Nat. Chem. Biol.*, **7**, 285–295.
22. Pattyn,F., Robbrecht,P., De Paepe,A., Speleman,F. and Vandesompele,J. (2006) RTPrimerDB: the real-time PCR primer and probe database, major update 2006. *Nucleic Acids Res.*, **34**, D684–D688.
23. Hellemans,J., Mortier,G., De Paepe,A., Speleman,F. and Vandesompele,J. (2007) qBase relative quantification framework and software for management and automated analysis of real-time quantitative PCR data. *Genome Biol.*, **8**, R19.
24. McPherson,A. (1982) *Preparation and Analysis of Protein Crystals*. Wiley, New York.
25. Kabsch,W. (2010) Integration, scaling, space-group assignment and post-refinement. *Acta Crystallogr. A*, **66**, 133–144.
26. Winn,M.D., Ballard,C.C., Cowtan,K.D., Dodson,E.J., Emsley,P., Evans,P.R., Keegan,R.M., Krissinel,E.B., Leslie,A.G., McCoy,A. *et al.* (2011) Overview of the CCP4 suite and current developments. *Acta Crystallogr. D*, **67**, 235–242.
27. McCoy,A.J., Grosse-Kunstleve,R.W., Adams,P.D., Winn,M.D., Storoni,L.C. and Read,R.J. (2007) Phaser crystallographic software. *J. Appl. Crystallogr.*, **40**, 658–674.

28. Langer,G., Cohen,S.X., Lamzin,V.S. and Perrakis,A. (2008) Automated macromolecular model building for X-ray crystallography using ARP/wARP version 7. *Nat. Protoc.*, **3**, 1171–1179.
29. Emsley,P. and Cowtan,K. (2004) Coot: model-building tools for molecular graphics. *Acta Crystallogr. D*, **60**, 2126–2132.
30. Afonine,P.V., Grosse-Kunstleve,R.W., Echols,N., Headd,J.J., Moriarty,N.W., Mustyakimov,M., Terwilliger,T.C., Urzhumtsev,A., Zwart,P.H. and Adams,P.D. (2012) Towards automated crystallographic structure refinement with phenix.refine. *Acta Crystallogr. D*, **68**, 352–367.
31. Chen,V.B., Arendall,W.B. 3rd, Headd,J.J., Keedy,D.A., Immormino,R.M., Kapral,G.J., Murray,L.W., Richardson,J.S. and Richardson,D.C. (2010) MolProbity: all-atom structure validation for macromolecular crystallography. *Acta Crystallogr. D*, **66**, 12–21.
32. Hubbard,S.J., Campbell,S.F. and Thornton,J.M. (1991) Molecular recognition. Conformational analysis of limited proteolytic sites and serine proteinase protein inhibitors. *J. Mol. Biol.*, **220**, 507–530.
33. McDonald,I.K. and Thornton,J.M. (1994) Satisfying hydrogen bonding potential in proteins. *J. Mol. Biol.*, **238**, 777–793.
34. Lee,T.I., Johnstone,S.E. and Young,R.A. (2006) Chromatin immunoprecipitation and microarray-based analysis of protein location. *Nat. Protoc.*, **1**, 729–748.
35. Gevry,N., Chan,H.M., Laflamme,L., Livingston,D.M. and Gaudreau,L. (2007) p21 transcription is regulated by differential localization of histone H2A.Z. *Genes Dev.*, **21**, 1869–1881.
36. Collavin,L., Lunardi,A. and Del Sal,G. (2010) p53-family proteins and their regulators: hubs and spokes in tumor suppression. *Cell Death Differ.*, **17**, 901–911.
37. Rothbauer,U., Zolghadr,K., Muyldermans,S., Schepers,A., Cardoso,M.C. and Leonhardt,H. (2008) A versatile nanotrap for biochemical and functional studies with fluorescent fusion proteins. *Mol. Cell. Proteomics*, **7**, 282–289.
38. Nooren,I.M. and Thornton,J.M. (2003) Diversity of protein-protein interactions. *EMBO J.*, **22**, 3486–3492.
39. Perkins,J.R., Diboun,I., Dessailly,B.H., Lees,J.G. and Orengo,C. (2010) Transient protein-protein interactions: structural, functional, and network properties. *Structure*, **18**, 1233–1243.
40. Wang,Y., Rosengarth,A. and Luecke,H. (2007) Structure of the human p53 core domain in the absence of DNA. *Acta Crystallogr. D*, **63**, 276–281.
41. Ory,K., Legros,Y., Auguin,C. and Soussi,T. (1994) Analysis of the most representative tumour-derived p53 mutants reveals that changes in protein conformation are not correlated with loss of transactivation or inhibition of cell proliferation. *EMBO J.*, **13**, 3496–3504.
42. Chen,Y., Dey,R. and Chen,L. (2010) Crystal structure of the p53 core domain bound to a full consensus site as a self-assembled tetramer. *Structure*, **18**, 246–256.
43. Lane,D.P. (1992) Cancer. p53, guardian of the genome. *Nature*, **358**, 15–16.
44. Vousden,K.H. and Prives,C. (2009) Blinded by the light: the growing complexity of p53. *Cell*, **137**, 413–431.
45. Harris,S.L. and Levine,A.J. (2005) The p53 pathway: positive and negative feedback loops. *Oncogene*, **24**, 2899–2908.
46. Lozano,G. (2010) Mouse models of p53 functions. *Cold Spring Harb. Perspect. Biol.*, **2**, a001115.
47. Berglind,H., Pawitan,Y., Kato,S., Ishioka,C. and Soussi,T. (2008) Analysis of p53 mutation status in human cancer cell lines: a paradigm for cell line cross-contamination. *Cancer Biol. Ther.*, **7**, 699–708.
48. Berns,K., Hijmans,E.M., Mullenders,J., Brummelkamp,T.R., Velds,A., Heimerikx,M., Kerkhoven,R.M., Madiredjo,M., Nijkamp,W., Weigelt,B. *et al.* (2004) A large-scale RNAi screen in human cells identifies new components of the p53 pathway. *Nature*, **428**, 431–437.
49. Vassilev,L.T., Vu,B.T., Graves,B., Carvajal,D., Podlaski,F., Filipovic,Z., Kong,N., Kammlott,U., Lukacs,C., Klein,C. *et al.* (2004) In vivo activation of the p53 pathway by small-molecule antagonists of MDM2. *Science*, **303**, 844–848.
50. Toledo,F. and Wahl,G.M. (2006) Regulating the p53 pathway: in vitro hypotheses, in vivo veritas. *Nat. Rev. Cancer*, **6**, 909–923.
51. Selivanova,G. and Wiman,K.G. (2007) Reactivation of mutant p53: molecular mechanisms and therapeutic potential. *Oncogene*, **26**, 2243–2254.
52. Yu,X., Vazquez,A., Levine,A.J. and Carpizo,D.R. (2012) Allele-specific p53 mutant reactivation. *Cancer Cell*, **21**, 614–625.
53. Liu,X., Wilcken,R., Joerger,A.C., Chuckowree,I.S., Amin,J., Spencer,J. and Fersht,A.R. (2013) Small molecule induced reactivation of mutant p53 in cancer cells. *Nucleic Acids Res.*, **41**, 6034–6044.
54. Arkin,M.R. and Wells,J.A. (2004) Small-molecule inhibitors of protein-protein interactions: progressing towards the dream. *Nat. Rev. Drug Discov.*, **3**, 301–317.
55. Komarov,P.G., Komarova,E.A., Kondratov,R.V., Christov-Tselkov,K., Coon,J.S., Chernov,M.V. and Gudkov,A.V. (1999) A chemical inhibitor of p53 that protects mice from the side effects of cancer therapy. *Science*, **285**, 1733–1737.
56. Komarova,E.A., Neznanov,N., Komarov,P.G., Chernov,M.V., Wang,K. and Gudkov,A.V. (2003) p53 inhibitor pifithrin alpha can suppress heat shock and glucocorticoid signaling pathways. *J. Biol. Chem.*, **278**, 15465–15468.
57. Rocha,S., Campbell,K.J., Roche,K.C. and Perkins,N.D. (2003) The p53-inhibitor pifithrin-alpha inhibits firefly luciferase activity in vivo and in vitro. *BMC Mol. Biol.*, **4**, 9.
58. Follis,A.V., Llambi,F., Ou,L., Baran,K., Green,D.R. and Kriwacki,R.W. (2014) The DNA-binding domain mediates both nuclear and cytosolic functions of p53. *Nat. Struct. Mol. Biol.*, **21**, 535–543.
59. Hagn,F., Klein,C., Demmer,O., Marchenko,N., Vaseva,A., Moll,U.M. and Kessler,H. (2010) BclxL changes conformation upon binding to wild-type but not mutant p53 DNA binding domain. *J. Biol. Chem.*, **285**, 3439–3450.
60. Vaseva,A.V. and Moll,U.M. (2009) The mitochondrial p53 pathway. *Biochim. Biophys. Acta*, **1787**, 414–420.
61. Pardon,E., Laeremans,T., Triest,S., Rasmussen,S.G., Wohlkonig,A., Ruf,A., Muyldermans,S., Hol,W.G., Kobilka,B.K. and Steyaert,J. (2014) A general protocol for the generation of Nanobodies for structural biology. *Nat. Protoc.*, **9**, 674–693.
62. Comel,A., Sorrentino,G., Capaci,V. and Del Sal,G. (2014) The cytoplasmic side of p53's oncosuppressive activities. *FEBS Lett.*, **588**, 2600–2609.
63. Delanote,V., Vanloo,B., Catillon,M., Friederich,E., Vandekerckhove,J. and Gettemans,J. (2010) An alpaca single-domain antibody blocks filopodia formation by obstructing L-plastin-mediated F-actin bundling. *FASEB J.*, **24**, 105–118.
64. Oren,M. and Rotter,V. (2010) Mutant p53 gain-of-function in cancer. *Cold Spring Harb. Perspect. Biol.*, **2**, a001107.